

# Cell-Based Ambient Venturi Autosampling and Matrix-Assisted Laser Desorption Ionization Mass Spectrometric Imaging of Secretory Products

Baojie Shen, Xiaoyu Yang, Sarah Elizabeth Noll, Xiaojie Yang, Yanping Liu, Shanshan Jia, Jiaying Zhao, Shi Zheng, Richard N Zare, and Hongying Zhong\*



Cite This: *Anal. Chem.* 2022, 94, 3456–3466



Read Online

ACCESS |



Metrics & More

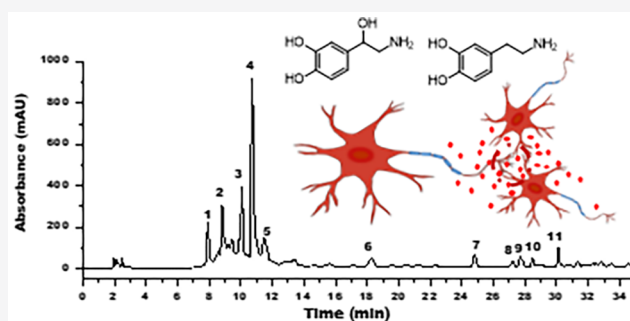


Article Recommendations



Supporting Information

**ABSTRACT:** A cell-based ambient Venturi autosampling device was established for the monitoring of dynamic cell secretions in real time with temporal resolution on the order of a second. Detection of secretory products of cells and screening of bioactive compounds are primarily performed on an ambient autosampling probe and matrix-assisted laser desorption ionization (MALDI) mass spectrometry. It takes advantage of the Venturi effect in which the fluid flowing through an inlet capillary tube is automatically fed into a parallel array of multiple outlet capillaries. Cells are incubated inside the inlet capillary tube that is connected with either a syringe pump or liquid chromatography (LC) for the transfer of single compounds or mixtures, respectively. Secretory products were continuously pushed into the outlet capillaries and then spotted into a compressed thin film of the matrix material 9-aminoacridine for MALDI mass spectrometric imaging. In physiological pH, without the use of high voltages and without the use of chemical derivatizations, this platform can be applied to the direct assay of neurotransmitters or other secretory products released from cells in response to the stimulation of individual compounds or LC-separated eluates of natural mixtures. It provides a new way to identify bioactive compounds with a detection limit down to 0.04 fmol/pixel.



## INTRODUCTION

Development of cell-based ambient autosampling devices that can sensitively transfer, quantify, and identify secretory products in real time with minimal disturbance to live cells is important for the dissection of interconnected cascades of intracellular signaling and aids in the development of novel therapeutic compounds.<sup>1–6</sup> Various spectroscopic or electrochemical techniques including enzyme-linked immunosorbent assay,<sup>7,8</sup> hyperspectral photonic crystal resonant imaging,<sup>9</sup> fluorescence imaging,<sup>10–12</sup> surface enhanced Raman spectroscopy,<sup>13–15</sup> as well as various electrochemical sensors,<sup>16–18</sup> and nanoplasmonic probes<sup>19</sup> have been established for quantitative and sensitive recording of targeted cell secretions with nanoscale temporal resolution.

Mass spectrometry is an alternative tool for the detection of cell secretions with not only temporal but also structural information.<sup>20–22</sup> The high sensitivity down to subfemtomolar or even the attomolar level along with accurate masses of ions makes it possible to elucidate diverse secretory products of cells. Electrospray ionization (ESI) has been a choice for continuous sampling and ionization of biomolecules. However, the spraying process is usually aided by a nebulizing gas (sometimes heated for efficient desolvation) and an electric field created between the spray capillary and the inlet of the

mass spectrometer. Electroporation or other disturbances to live cells are a concern in the application of high voltages, acidic/basic solvents, and heated nebulizing gases. These technical challenges have kept driving the elaboration of this technique. Taking advantage of the Venturi effect, several autoupumping devices have been developed for the transfer of various samples to mass spectrometers.<sup>23–25</sup> Compared with the sampling of air contaminants<sup>26</sup> or screening of enzyme inhibitors,<sup>27</sup> the detection of secretory products of live cells requires efficient ionization under physiological conditions at near neutral pH without the application of high voltages. Sonic spray ionization is an alternative without the use of a high voltage.<sup>28–32</sup> Although a sheath gas flow at sonic speed can create a statistical imbalance of charges on droplets which eventually create gaseous ions, the smaller number of charged species compared to the high voltage-driven ESI limits the

**Received:** August 23, 2021

**Accepted:** February 2, 2022

**Published:** February 14, 2022



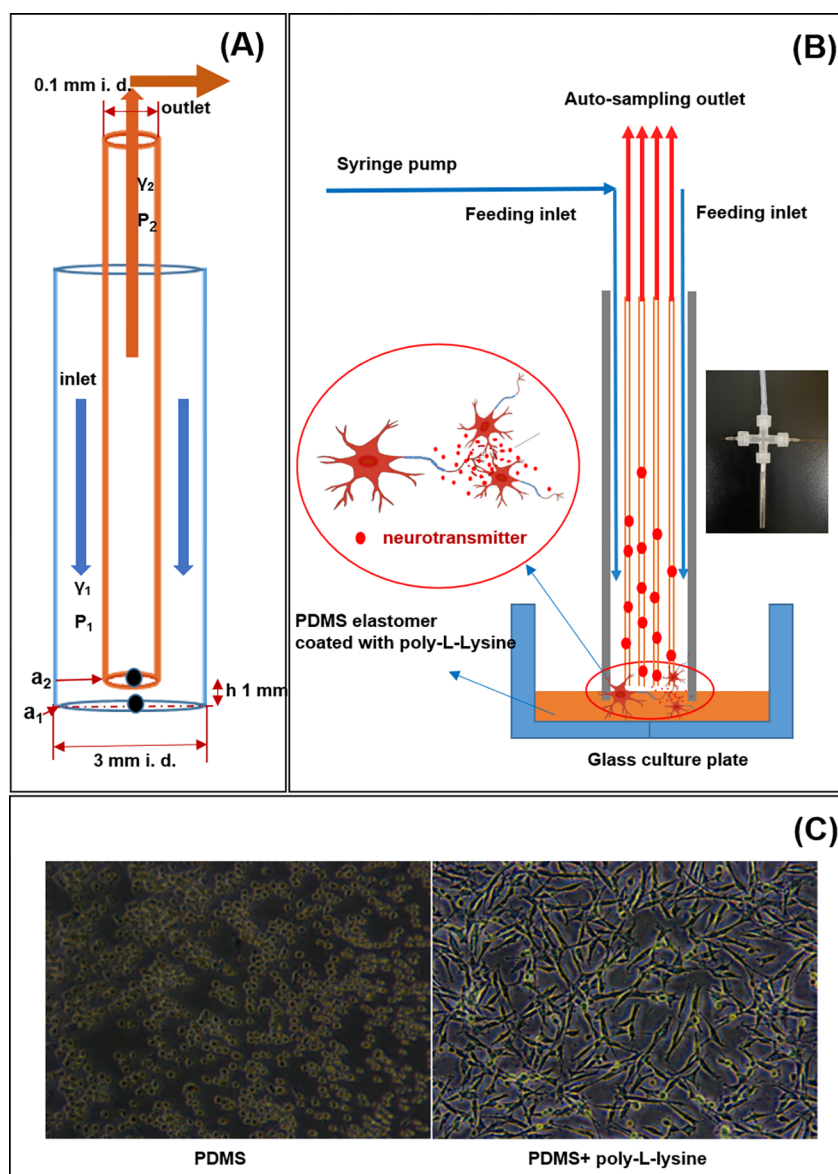


**Figure 1.** Design of the cell-based ambient Venturi autosampling device. (A) Flow diagram of the fluid. (B) Layout of multiple outlets and the coupling to a culture plate. (C) Optical images of PC12 cells on PDMS modified culture plates without or with poly-L-lysine coatings. *P*, Pressure; *a*, Area; *h*, Height;  $\gamma$ , Velocity; 1, inlet; 2, outlet.

detection of low-abundance substances.<sup>33–35</sup> Importantly, because ion losses in the nonfocused spraying plume are unavoidable in all spraying techniques, new methods are needed for quantitative and sensitive monitoring of the kinetics of intercellular secretions.

Herein, we describe an ambient autosampling device coupled with a matrix-assisted laser desorption ionization (MALDI) mass spectrometer. In contrast to spraying techniques by which only a fraction of the sample is measured, our method better captures all types of ions, by integrating intensities across the image of a spotted sample. This approach reduces ion losses and achieves quantification of cell-released compounds. For a proof-of-principle demonstration, this method was applied to the mass spectrometric imaging of neurotransmitters such as dopamine and norepinephrine<sup>36–38</sup> as well as other secretory products released from PC12 cells in response to the stimulation of KCl, eight bioactive compounds, and green tea and *Veratrum nigrum* L extracts.

## EXPERIMENTAL SECTION

**Modification of Cell Culture Plates.** Reagents and apparatus are described in *Notes S1*. Surfaces of glass culture plates have been chemically modified with polydimethylsiloxane (PDMS) elastomer so as to ensure sealing when the Venturi probe is placed on the plate. The tight seal between the outer capillary of the Venturi probe and the plate is crucial for generating the pressure differences needed to pump out the secretory products of cells through the inner capillaries. The SYLGARD 184 silicone elastomer base (1.745 mL) was mixed with the solution of the SYLGARD 184 silicone elastomer curing agent (0.1745 mL) in a beaker. The mixture was gently poured into a glass culture plate so as to avoid formation of any air bubbles. The plate was then put in an oven to heat at 80 °C for 30 min. The resultant layer of PDMS is about 2 mm thick with a diameter of 35 mm. Because of the hydrophobicity of the PDMS layer, on which it is difficult to grow PC12 cells, the PDMS layer was further coated with poly-L-lysine. The stock

solution of concentrated poly-L-lysine 0.1% (w/v) was diluted 10-fold with sterilized water. The PDMS-coated culture plate was then soaked in the diluted poly-L-lysine solution for 5 min before the solution was poured out of the plate. The plate was air-dried at room temperature overnight. It was rinsed with sterilized water three times and then stored at 4 °C. Before further use, plates were exposed to UV irradiation for thorough sterilization.

**Establishment of the Ambient Venturi Autosampling Device.** The device consists of three parts including a coated cell culture plate, a wide glass inlet (inner diameter: 3 mm; outer diameter: 4 mm) connected to a Harvard pump, and one or multiple fused silica capillary outlets (inner diameter: 100  $\mu\text{m}$ , 150  $\mu\text{m}$ , and 320  $\mu\text{m}$ ; outer diameter: 365  $\mu\text{m}$ ) assembled inside the wide glass inlet. The solvent flowing inside the wide glass inlet was pumped at 20  $\mu\text{L}/\text{min}$  to flush out secretory cell products. Eluates from the capillary outlet were collected and mass-analyzed. To assess device performance, a solution of Gentian violet was prepared with pure water at a concentration of 2.5 mg/mL. A drop of either 0.5 or 2  $\mu\text{L}$  of the Gentian violet solution was placed on the surface of the coated cell culture plate for sampling with one- or four-outlet capillaries, respectively. Eluted solutions were collected on a paper every second. The amount of Gentian violet in each air-dried eluted spot was semiquantified with Image J software.<sup>39</sup> A Waters Synapt G2 (Milford, MA, USA) MALDI mass spectrometer was used for the detection of secretory products of PC12 cells. Cultivation and stimulation of PC12 cells, instrumental calibration of the mass spectrometer and quantification procedures, and the enrichment of secretory dopamine and norepinephrine are described in Notes S2–S4, respectively. In regular MALDI mass spectrometry, the co-crystallization of analytes and matrix materials usually results in non-uniform crystal sizes and shapes. Acquired signal intensities may vary from spots to spots. In this work, the quantification was enhanced by two means:

- (1) Samples were not mixed with the solution of matrix materials. Instead, matrix materials such as (dimethylamino) naphthalene (DMAN) or 9-aminoacridine (9-AA) were compressed into a uniform thin film on the sticky side of aluminum tape. The aluminum tape was then put on a stainless steel sample plate for MALDI imaging. Samples were spotted on the uniform thin film of DMAN or 9-AA. This sampling procedure improves the crystallization process.
- (2) Signal intensities were not acquired from a single spot or averaged multiple spots. Instead, the laser beam scanned across the whole areas of sample spots. Signal intensities were integrated, which means that signal intensities from all spots were added together. This data handling mode significantly decreases the spot-to-spot variations. Figure S1 shows that equal amounts of samples spotted on the same thin film of 9-AA generate equivalent integrated signal intensities with a relative variation of  $\sim 1\%$ .

## RESULTS AND DISCUSSION

**Design of the Cell-Based Ambient Venturi Autosampling Device.** The key features of the cell-based ambient autosampling Venturi device are the continuous transfer of chemical compounds to stimulate cells and online collection of secretory products of live cells for mass spectrometric imaging. Figure 1A shows the flow diagram of the fluid in autosampling

Venturi device. The wider feeding inlet carries the KR buffer which exits through the narrower inner capillary. According to well-known Bernoulli's theory (Note S5),<sup>40</sup> pressure differences ( $P_1 - P_2$ ), capillary cross sections, and the height of the autopumping outlet above the culture plate determine the velocity of the outlet fluid. In this work, pressure differences are determined by the syringe pump that moves the fluid to flow through the feeding inlet, as well as the backpressure of the outlet capillary. High pressure differences ( $P_1 - P_2$ ), wide feeding inlet capillary ( $a_1$ ), narrow autopumping outlet ( $a_2$ ), and low height ( $h$ ) lead to a high velocity that can rapidly flush out secretory products of cells (Note S6). It should be noted that higher pressures may detach cells from the plate. In particular, when the height of the narrow outlet capillary is too low and too close to the plate, cell debris usually causes clogging of the narrow outlet capillary. However, too large a height broadens the elution profile and leads to very low recovery (Figure S2). The diameter of the narrow outlet capillary has been optimized to improve the detection and response time. Considering  $\sim 10^6$  cells in a culture plate with a diameter of 35 mm, it has been estimated that there are  $\sim 9000$  cells under a wide inlet capillary with a diameter of 3 mm but only  $\sim 10$  cells under a narrow outlet capillary with a diameter of 100  $\mu\text{m}$ . To achieve both high velocity and high sensitivity, multiple autopumping outlet capillaries were installed in parallel inside the wide feeding inlet capillary as shown in Figure 1B.

The connection of the Venturi probe to cell culture plates requires a tight seal that is crucial for building up pressure differences. It has been experimentally demonstrated that the direct contact of glass Venturi probes with glass culture plates is not able to generate any Venturi effects because of leaking. Taking advantage of the elasticity of PDMS, the Venturi probe can be sufficiently sealed to the modified surface of the glass culture plate. However, because of the strong hydrophobicity of PDMS, PC12 cells were not able to attach and grow as shown in Figure 1C. The attachment, growth, and development of cells are typically dependent on many attachment factors and extracellular matrix components. For those cells that are not able to synthesize sufficient attachment factors, exogenous sources are required. The coating of poly-L-lysine provides positive lysine sites at physiological pH that enhances electrostatic interactions with negative ions on the surface of the cell. Figure 1C shows well-developed PC12 cells on poly-L-lysine-coated PDMS surfaces. Figure S3 shows that the modification of cell culture plates with PDMS and poly-L-lysine does not affect the secretion of PC12 cells. Equal amounts of dopamine and norepinephrine were detected from the supernatants of cell culture plates with or without PDMS and poly-L-lysine modification.

**Assessment and the Coupling of the Venturi Probe to the Mass Spectrometer.** The performance of the home-built device was assessed by the response time, recovery, and sensitivity. The response time is directly associated with the velocity of the outlet fluid. As expected, the narrower the autopumping outlet ( $a_2$ ), the faster the velocity of the liquid so that the secretory products of cells are rapidly flushed out. Using Gentian violet dye (2.5 mg/mL in water), we have visualized the transportation of molecules through the autopumping outlets. As shown in Figure S4A and Video S1, a droplet of Gentian violet was put on the surface of the cell culture plate. It was either 0.5 or 2.0  $\mu\text{L}$  for the system with one-outlet capillary or four-outlet capillaries. Outlet capillaries

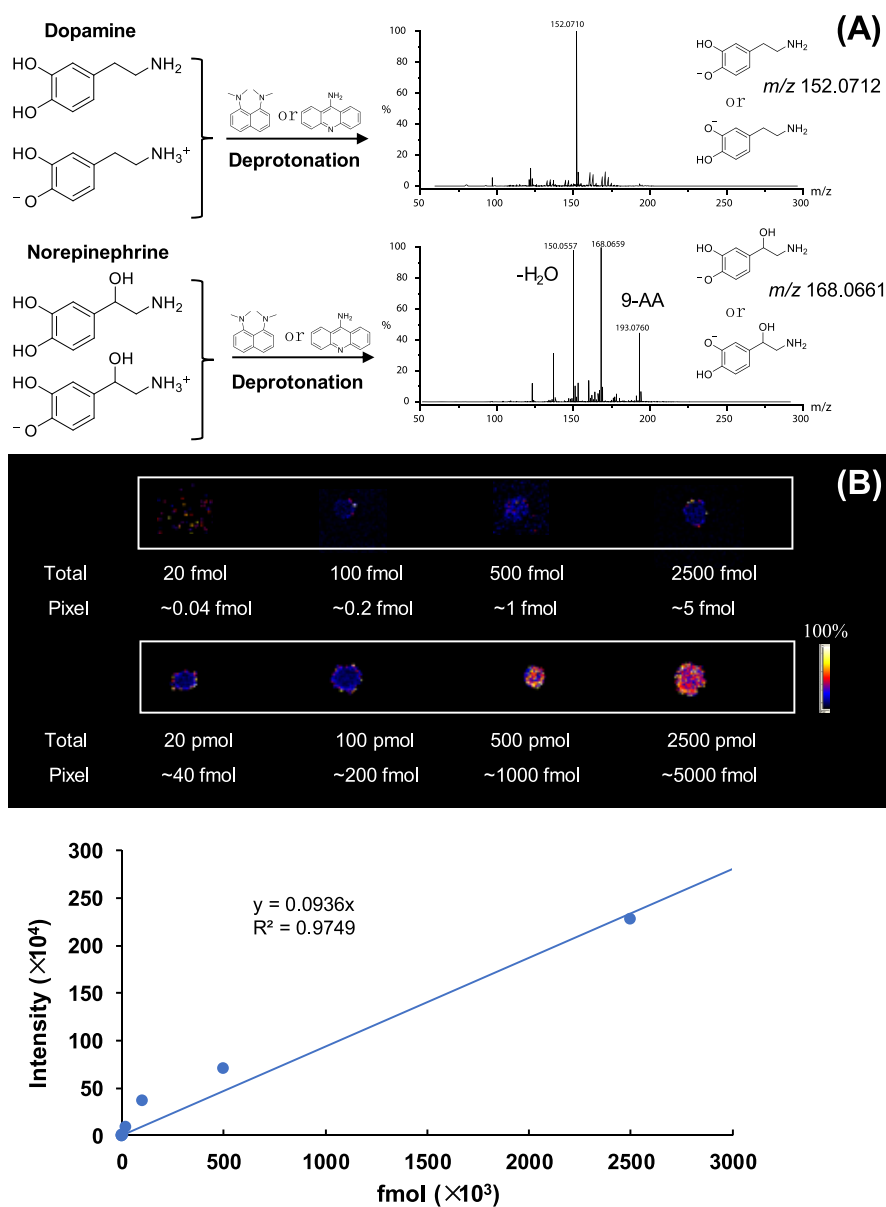


**Figure 2.** MALDI mass spectrometric imaging with basic matrix materials. (A) Mass spectra of deprotonated dopamine and norepinephrine. (B) Detection limit and quantitative correlation of intensities with quantities.

with different inner diameters have been assessed including narrow (ID: 100  $\mu\text{m}$  and OD: 365  $\mu\text{m}$ ), medium (ID: 150  $\mu\text{m}$  and OD: 365  $\mu\text{m}$ ), and wide (ID: 320  $\mu\text{m}$  and OD: 450  $\mu\text{m}$ ) for the transportation of the dye. Our data show that the response time varies with the inner diameter of the outlet capillary. When 0.5  $\mu\text{L}$  of Gentic violet was spotted on the surface of the culture plate, it took 3, 4, and 6 s to observe dye-containing eluates for outlet capillaries with 100, 150, and 320  $\mu\text{m}$  inner diameters, respectively. Eluates were quantified by optical densities of dye fractions. Within 10 s, resultant recoveries are 87, 81, and 44% for outlet capillaries with 100, 150, and 320  $\mu\text{m}$  inner diameters, respectively. It was shown that the wide inner diameter of the outlet capillary leads to slow fluid velocity, a wide band width, and low recovery. The low recovery may result from lateral diffusion inside the capillary. It was then proposed that the recovery should be improved if the lateral diffusion could be controlled. Four-outlet capillaries with 100  $\mu\text{m}$  inner diameter were put at four

different locations on the spot as shown in Figure S4B. To compare the four-outlet system with the previous one-outlet system, 2.0  $\mu\text{L}$  instead of 0.5  $\mu\text{L}$  of Gentic violet was spotted on the surface of the culture plate. It was found that the fluid velocity was dramatically increased, and the efficiency of transportation was improved. About 83% of the dye was recovered in the spot collected at 2 s and 96% eluted within 10 s. These experimental results indicate that the blank time of the four-outlet system is 1 s, which leads us to deduct 1 s from the observed time. Figure S4B also indicates that the system containing four-outlet capillaries has a much more centralized elution profile. With computer-controlled automatic fractionation of eluates, it should be possible to collect eluates with very high temporal resolution, down to milliseconds (ms), for transient studies in the future. This work was focused on long-lasting experiments in which eluates were collected at time intervals ranging from a few seconds to several minutes.

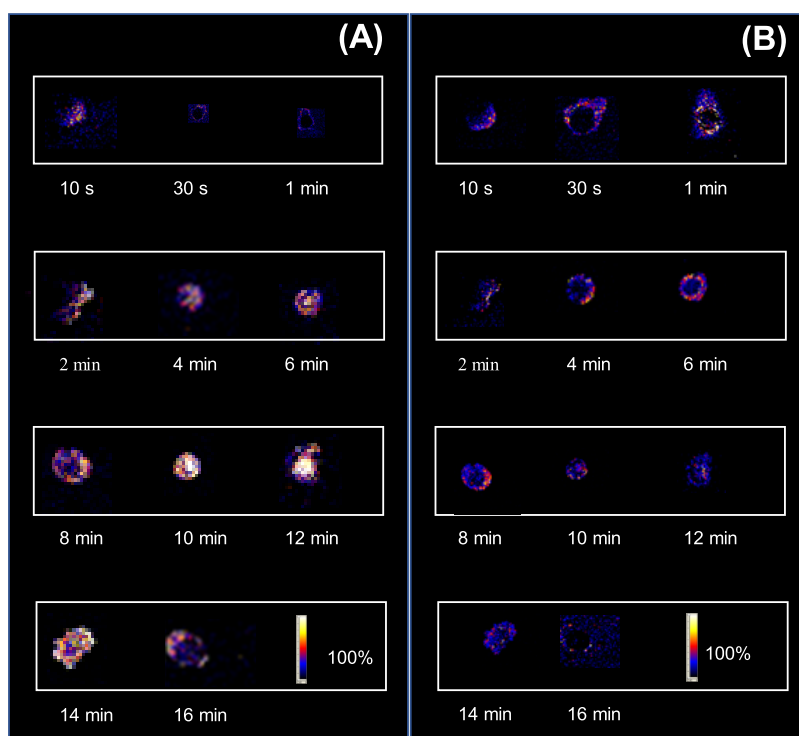


**Figure 3.** MALDI mass spectrometric imaging of secretory products of PC12 cells in response to the stimulation of KCl. (A) Dopamine. (B) Norepinephrine.

Important neurotransmitters were tested as representative secretory products of PC12 cells. Ambient ESI has been a well-recognized technique for real-time monitoring of secretory products of cells.<sup>41–43</sup> Because it requires high voltage, up to 3–6 kV, cell lysates resulting from rapid electroporation of cells may interfere with the detection of secretory species. However, in the absence of high voltages (Videos S2 and S3) and under near neutral pH physiological conditions, only noise was observed in the mass spectra. This work selects MALDI for rapid screening of cell responses, enabling simultaneous visualization of multiple components and avoiding ion losses. Mass spectrometric detection of neurotransmitters such as dopamine and noradrenaline is usually not sensitive because of the formation of uncharged zwitterions<sup>44</sup> or neutral phenolic amine species.<sup>45</sup> Figure S5 and Videos S2 and S3 show that dopamine (10 mg/mL) was not detected in either positive or negative ion modes using regular MALDI or ESI at neutral pH without the application of high voltages, respectively. Naccarato et al. reported a gas chromatography–triple quadrupole mass spectrometry approach for rapid analysis of dopamine and noradrenaline in human urine after a fast derivatization of both aliphatic amino and phenolic moieties by propyl chloroformate.<sup>46</sup> Other chemical reagents including 4-(anthracen-9-yl)-2-fluoro-1-methylpyridin-1-ium iodide and 2,4-diphenylpyrylium were reported for the chemical derivatization of –OH or –NH<sub>2</sub> groups of neurotransmitters to generate positive ions in MALDI mass spectrometric analysis.<sup>47,48</sup> We propose herein a direct MALDI analysis approach without any chemical derivatization. It is based on the principle of the deprotonation reaction of phenolic hydroxyl groups with strong organic bases such as 1,8-bis(dimethylamino)naphthalene (DMAN, a so-called proton sponge) and 9-AA. As shown in Figure 2A, uncharged zwitterions or neutral phenolic amine species are deprotonated and detected at a bias

voltage of 5 V. Other catecholamine neurotransmitters, such as epinephrine, as well as 5-hydroxytryptamine,  $\gamma$ -aminobutyric acid, glycine, glutamic acid, and serine, can all be deprotonated and analyzed with the proposed approach as shown in Figure S6. Because DMAN evaporates rapidly under high vacuum (Figure S7), 9-AA was eventually chosen for MALDI analysis. It has been demonstrated that the matrix film of 9-AA remains intact while DMAN has completely evaporated in the vacuum after several hours of MALDI imaging experiments. Because dopamine is prone to oxidation under basic conditions, we have investigated mixing samples with antioxidants such as sodium pyrosulfate. However, the oxidized products were not observed under the high vacuum of the mass spectrometer because of the absence of oxygen, from which we conclude that it is safe to use 9-AA as a matrix material for MALDI analysis of these neurotransmitters. Extensive fragmentations of these fragile molecules were observed at 20 V bias voltage as shown in Figure S8. The detection limit of dopamine can be down to 0.04 fmol/pixel and mass spectrometric intensities are in good accordance with total quantities ranging from 20 fmol to 2500 pmol as shown in Figure 2B. Similar results were obtained for noradrenaline in Figure S9.

**Detection of Secretory Products of PC12 Cells.** As a well-established model for studies of the neuronal secretion, PC12 cells can synthesize dopamine and limited amounts of noradrenaline that are stored in large dense-core vesicles. The release of these neurotransmitters is activated upon the depolarization in a Ca<sup>2+</sup>-dependent exocytotic pathway.<sup>48</sup> Neurotransmitter-containing vesicles dock on the cell membrane before releasing these chemical messengers by fusion of the vesicle to the cell membrane.<sup>49</sup> Mass spectrometric detection of secreted neurotransmitters with temporal resolution provides a sensitive way to investigate biological activities such as the opening of sodium channels for sufficient

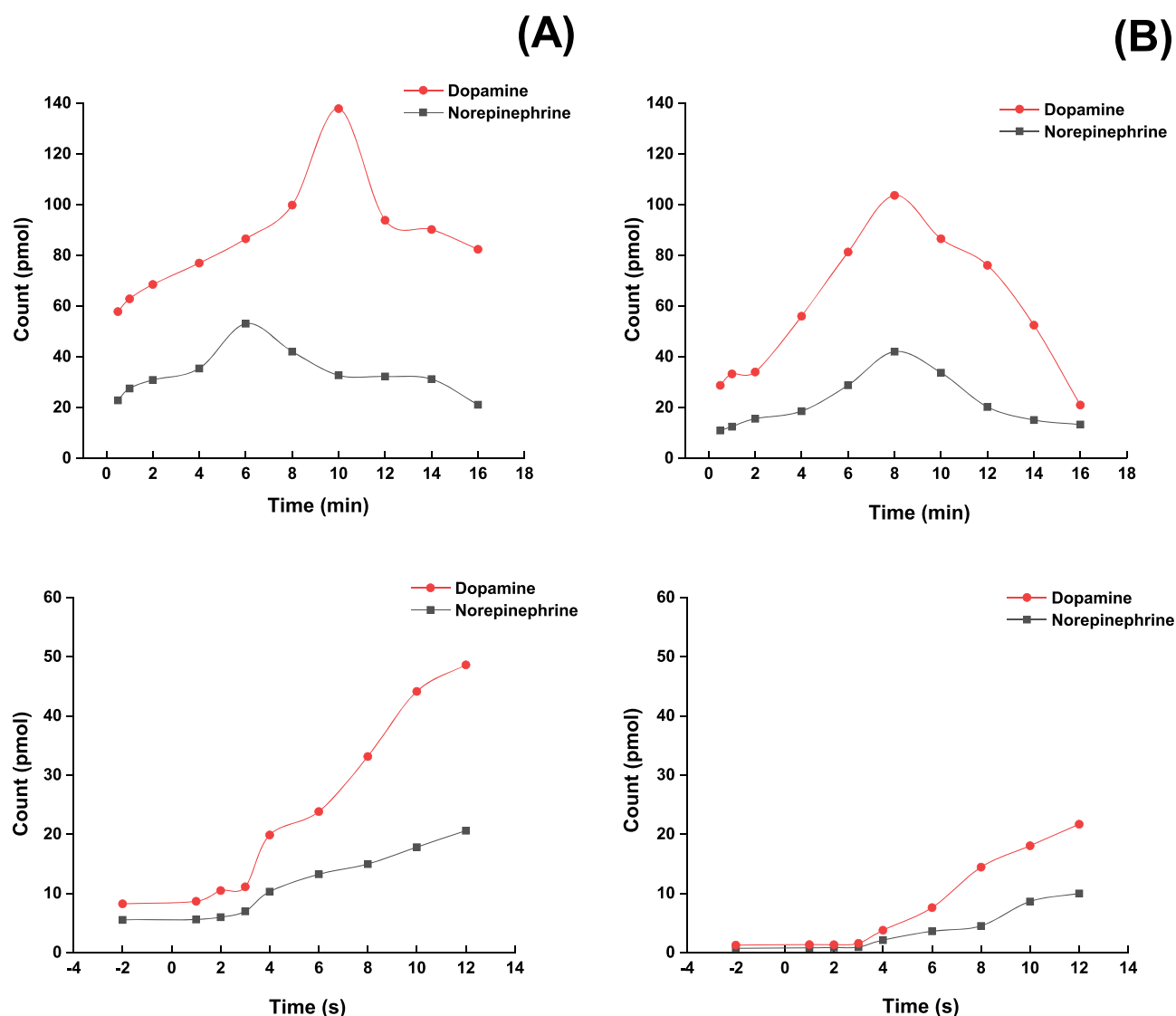


Figure 4. Comparison of dynamic secretions of PC12 cells to different chemical stimulation. (A) KCl. (B) Drug veratridine.

depolarization of the cell membrane, the subsequent opening of voltage-sensitive calcium channels, G-protein coupling with receptor proteins, and other potential rate-limiting mechanisms. This device was applied to monitor dynamic responses of PC12 cells under chemical stimulations. Figures S10 and S11 illustrate that PC12 cells cannot survive 2 h of stimulation with 60 mM KCl and  $10^{-4}$  M veratridine. All downstream experiments were completed within 30 min using well-grown cells. Figure 3 represents mass spectrometric detection of secreted dopamine and noradrenaline at different time intervals in response to the stimulation with 60 mM KCl.

Figure 4A summarizes that quantities of secreted dopamine and noradrenaline are similar within the first 3 s but start to increase afterward under the KCl stimulation. Deducting 1 s of dead volume time, latencies of stimulation-released secretions of dopamine and noradrenaline are about 3 s. Three experimental facts have been noted under the stimulation with KCl. First, the quantity of secreted dopamine of PC12 cells is greater than that of noradrenaline. This is in accordance with a previous report.<sup>49</sup> PC12 cells mainly synthesize dopamine along with limited noradrenaline. Second, there are obvious secretion peaks for dopamine and noradrenaline of

which noradrenaline is 4 min ahead of dopamine. As we know, noradrenaline is synthesized from dopamine by  $\beta$ -hydroxylase. It has been reported that KCl stimulation also promotes noradrenaline transporter function in PC12 cells in addition to boosting release of noradrenaline.<sup>50</sup> The noradrenaline transporter plays a vital role in terminating noradrenergic transmission by ferrying noradrenaline back into the cytoplasm following release.<sup>50</sup> This fact may explain why the secretion of noradrenaline starts to decrease while the secretion of dopamine is still increasing. Third, even after 16 min of stimulation, secreted dopamine and noradrenaline still remain at high levels, about 80 and 20 pmol, respectively. This experimental result proves the presence of a steady-state elevation of  $\text{Ca}^{2+}$  during prolonged depolarization with high KCl that continuously triggers exocytosis.<sup>51</sup> All these findings indicate that the cell-based device is useful for investigating long-lasting biological events in the timescale of seconds or even minutes in contrast to transient spikes at ms levels.

Figure 4B shows that the drug veratridine produces different release characteristics. Caused by the opening of sodium channels, it was reported that the application of veratridine causes sufficient depolarization of the cell membrane to open

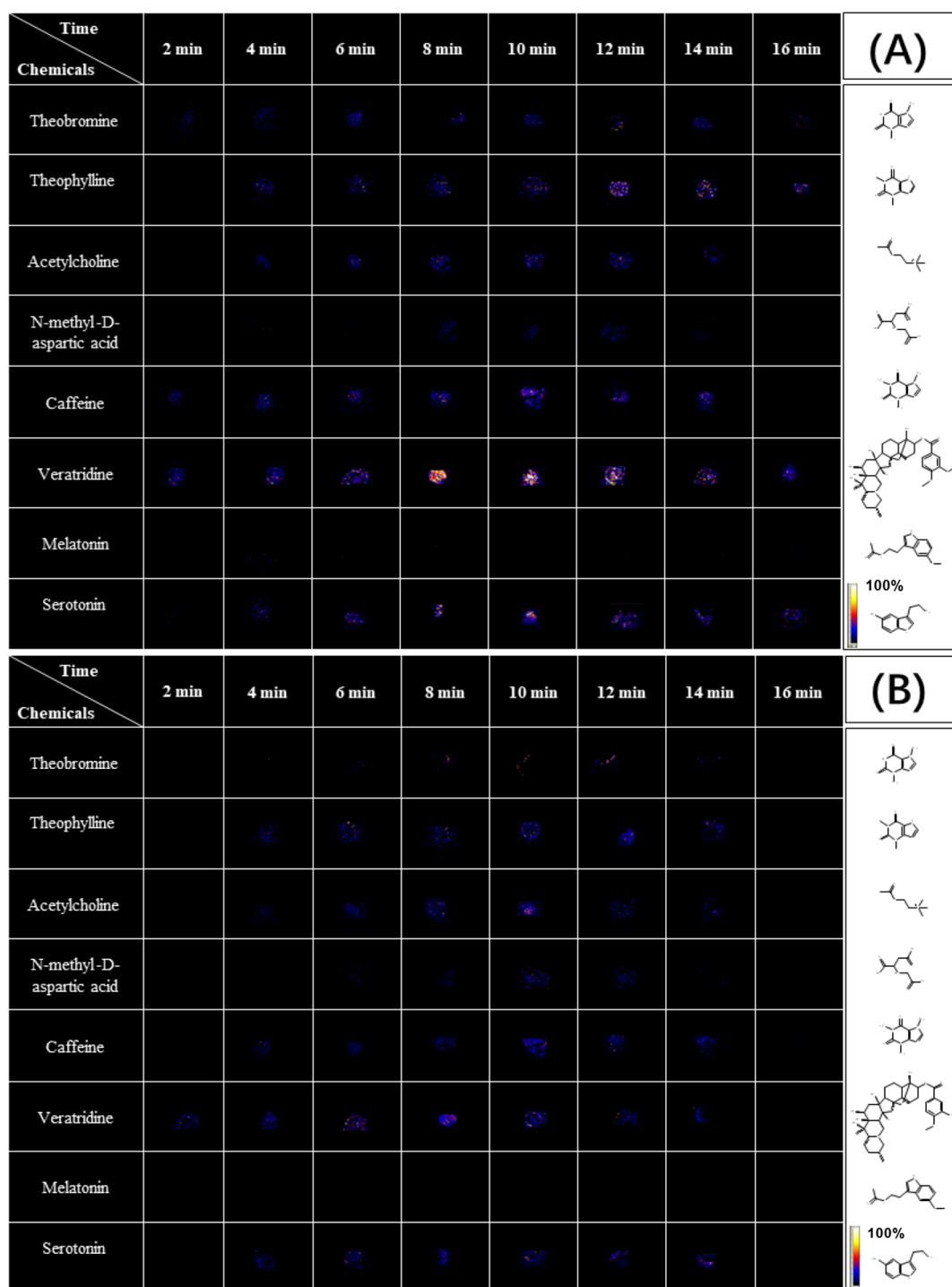


**Figure 5.** MALDI mass spectrometric imaging of secretory products of PC12 cells in response to 8 chemical stimulants. (A) Dopamine. (B) Norepinephrine.

voltage-sensitive calcium channels and subsequent exocytosis.<sup>52</sup> It was shown in Figure 4B that secreted noradrenaline tracks with dopamine upon the stimulation of veratridine, unlike the profiles observed with KCl stimulation. It seems that veratridine stimulation does not promote noradrenaline transporter function in PC12 cells as KCl does. Additionally, the high levels of dopamine and noradrenaline maintained in prolonged depolarization with KCl were also not observed. After 16 min of stimulation, both dopamine and noradrenaline dropped down to original levels.

Figure 5, shows images of dopamine and noradrenaline secreted from PC12 cells and collected at different time intervals in response to stimulations with eight bioactive compounds, including theobromine, theophylline, acetylcholine chloride, *N*-methyl-D-aspartic acid (NMDA), caffeine, veratridine, melatonin, and serotonin. It was found that there are no detectable dopamine and noradrenaline with treatment of NMDA or melatonin. Although NMDA has been recognized as an excitatory neurotransmitter that may activate the release of dopamine, this work corroborates the finding

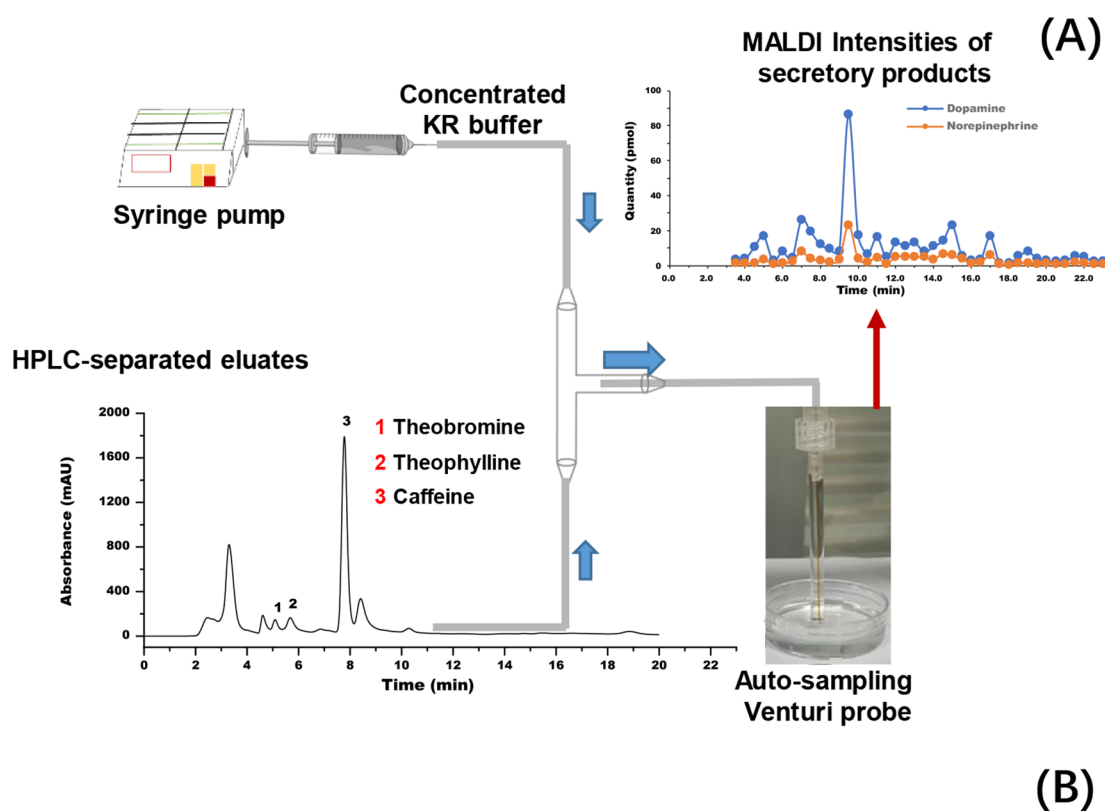


**Figure 6.** MALDI mass spectrometric detection of secretory products of PC12 cells in response to tea extracts. (A) HPLC separation coupled to the ambient Venturi autosampling probe. (B) Imaging of secreted dopamine.

that PC12 cells lack functional expression of NMDA receptors.<sup>53</sup> Inhibition of dopamine release by melatonin is not surprising. In 1983, Zisapel and Laudon reported that inhibition by melatonin may originate from the reduction of calcium ion release.<sup>54</sup> Among the eight compounds, caffeine was found to be the second strongest compound next to veratridine in terms of dopamine release by antagonizing the

effects of endogenous adenosine.<sup>55</sup> Secreted dopamine and noradrenaline were also detected under the stimulation of acetylcholine chloride, serotonin, theobromine, and theophylline with similar structures of which the underlying mechanisms are not known.

**Coupling to High-Performance Liquid Chromatography (HPLC) for Bioactivity Screening of Complex**



**Mixtures.** This new cell-based ambient autosampling device has been applied to the fast and efficient identification of bioactive lead compounds in complex natural mixtures. Coupling of the autosampling Venturi device to HPLC allows the separation of the mixtures of natural products. Figure S12 illustrates the reproducibility of the system for the analysis of natural products. HPLC-separated eluates were online mixed with a concentrated KR buffer that was transported with a syringe pump to dilute the organic solvent and maintain physiological conditions for PC12 cells. Figure 6A shows a chromatogram of green tea extracts in which three major components are labeled, including theobromine, theophylline, and caffeine. Secretory products from the outlet capillaries were collected at 30 s intervals and spotted on a thin film made of the 9-AA matrix material for MALDI mass spectrometric imaging. Two representative secretory products of PC12 cells including dopamine and norepinephrine are shown in Figures 6B and S13, respectively. Mass spectrometric intensities of each spot collected at different times were plotted in comparison with the chromatogram. It was found that PC12 cells respond to most components of tea extracts, in particular for caffeine. This system has also been applied to more complex mixtures of *Veratrum nigrum* L extracts (Figure S14).<sup>56</sup> Identified compounds are listed in Table S2. Peak values of dopamine and norepinephrine were observed slightly after the elution of angeloylzygadenine, veratrosine, jervine, veratramine, and veratridine. Among these, veratramine is the major alkaloid from *Veratrum nigrum* L. It has been well recognized as a good membrane permeant, the blocker of Na<sup>+</sup> channels, and prone to undergo rapid passive diffusion.<sup>57</sup> The underlying mechanism of veratramine-induced secretion of dopamine and norepinephrine of PC12 cells remains unknown. When HPLC is coupled with the autosampling Venturi probe, an important issue should be noted: HPLC-separated eluates are continuously pumped to cells and some of them may be coeluted. Then the stimulation time of components is transient and dependent on peak widths. Detected cell responses may result from synergistic effects of multiple compounds, in particular for those cells that have a slow response to some compounds.

## CONCLUSIONS

It has been shown that the combination of a Venturi probe and MALDI imaging provides a new cell-based technique for the screening of secretory products of cells in response to different chemical or pharmacological stimulations. The home-built ambient autosampling device can continuously transport stimulants to the targeted cells and collect secretory products at second intervals, which may be shortened further in the future. MALDI imaging with basic organic compound 9-AA as a matrix material makes it possible to quantitatively measure neurotransmitters that are difficult to detect with regular ESI. The coupling of this system to HPLC allows the screening of bioactive compounds from complex mixtures of natural products.

## ASSOCIATED CONTENT

### Supporting Information

The Supporting Information is available free of charge at <https://pubs.acs.org/doi/10.1021/acs.analchem.1c03625>.

Video S1: Fractionation of the dye (MP4)

Video S2: Spraying based on the Venturi effect (MP4)

Video S3: Ultrasonic spraying based on the Venturi effect (MP4)

Note S1: Reagents and apparatus; Note S2: Cultivation and stimulation of PC12 cells; Note S3: Instrumentation and calibration of the mass spectrometer; Note S4: Enrichment of secretory dopamine and norepinephrine; Note S5: The theoretical illustration of Venturi effects; Note S6: The effects of height and syringe pumping speed to velocity and recovery of Venturi autosampling. Figure S1: Quantification with the proposed MALDI technique. Figure S2: The Venturi autosampling of Gentian violet at a height of 5 mm; Figure S3: No effects of PDMS and poly-L-lysine coating on PC12 cell secretion; Figure S4: The dependence of response time and recovery on diameters of outlets; Figure S5: Mass spectra of dopamine with MALDI using different matrix materials; Figure S6: Mass spectrometric analysis of catecholamine neurotransmitters; Figure S7: Optical images of matrix materials used for MALDI analysis of neurotransmitters; Figure S8. Mass spectra of dopamine and noradrenaline at 20 V high bias voltages; Figure S9: Quantitative assessment of the MALDI analysis of neurotransmitters with 9-AA as matrix materials; Figure S10. Images of PC12 cells stimulated with 60 mM KCl; Figure S11: Images of PC12 cells stimulated with 0.0010 M veratridine; Figure S12: Assessment of the reproducibility of the system for analysis of natural products; Figure S13. MALDI mass spectrometric imaging of secreted norepinephrine of PC12 cells in response to HPLC-separated tea extracts; Figure S14: Bioactivity screening of the complex mixtures of *Veratrum nigrum* L extracts. Table S1: Preparation of KR buffer and KR buffer containing concentrated KCl (60 mM) or a Na<sup>+</sup> ion channel opener veratridine (0.1 mM); Table S2. Identified compounds from *Veratrum nigrum* L extracts (PDF)

## AUTHOR INFORMATION

### Corresponding Author

**Hongying Zhong** – Laboratory of Mass Spectrometry, College of Chemistry, Key Laboratory of Pesticides and Chemical Biology, Central China Normal University, Ministry of Education, Wuhan, Hubei 430079, P. R. China; State Key Laboratory for Conservation and Utilization of Subtropical Agro-Bioresources, College of Life Science and Technology, Guangxi University, Nanning, Guangxi 530004, P. R. China; [orcid.org/0000-0003-2733-7909](https://orcid.org/0000-0003-2733-7909); Phone: 86-13545053652; Email: [hyzhong@gxu.edu.cn](mailto:hyzhong@gxu.edu.cn)

### Authors

**Baojie Shen** – Laboratory of Mass Spectrometry, College of Chemistry, Key Laboratory of Pesticides and Chemical Biology, Central China Normal University, Ministry of Education, Wuhan, Hubei 430079, P. R. China

**Xiaoyu Yang** – Laboratory of Mass Spectrometry, College of Chemistry, Key Laboratory of Pesticides and Chemical Biology, Central China Normal University, Ministry of Education, Wuhan, Hubei 430079, P. R. China

**Sarah Elizabeth Noll** – Department of Chemistry, Stanford University, Stanford, California 94305, United States

**Xiaojie Yang** – Laboratory of Mass Spectrometry, College of Chemistry, Key Laboratory of Pesticides and Chemical

Biology, Central China Normal University, Ministry of Education, Wuhan, Hubei 430079, P. R. China

**Yanping Liu** – Laboratory of Mass Spectrometry, College of Chemistry, Key Laboratory of Pesticides and Chemical Biology, Central China Normal University, Ministry of Education, Wuhan, Hubei 430079, P. R. China

**Shanshan Jia** – Laboratory of Mass Spectrometry, College of Chemistry, Key Laboratory of Pesticides and Chemical Biology, Central China Normal University, Ministry of Education, Wuhan, Hubei 430079, P. R. China

**Jiaxing Zhao** – State Key Laboratory for Conservation and Utilization of Subtropical Agro-Bioresources, College of Life Science and Technology, Guangxi University, Nanning, Guangxi 530004, P. R. China

**Shi Zheng** – Laboratory of Mass Spectrometry, College of Chemistry, Key Laboratory of Pesticides and Chemical Biology, Central China Normal University, Ministry of Education, Wuhan, Hubei 430079, P. R. China

**Richard N Zare** – Department of Chemistry, Stanford University, Stanford, California 94305, United States;

orcid.org/0000-0001-5266-4253

Complete contact information is available at:

<https://pubs.acs.org/10.1021/acs.analchem.1c03625>

### Author Contributions

H.Z. and R.N.Z. developed the original concept, designed experiments, analyzed data, and wrote the manuscript. B.S. and X.Y. set up the system and performed experiments of sample preparation, HPLC, cell growth, and MALDI mass spectrometry. S.E.N. contributed to the establishment and performed some ESI experiments. X.Y. and Y.L. were involved in the work of natural products. S.J. and S.Z. were involved in the work of MALDI. J.Z. has been involved in data analysis.

### Notes

The authors declare no competing financial interest.

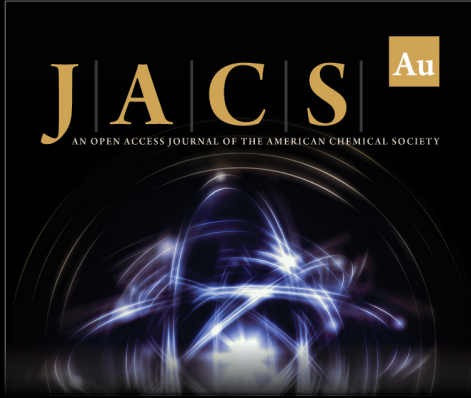
## ACKNOWLEDGMENTS

The authors acknowledge the financial support from the National Natural Science Foundation of China (NSFC 81761128005 and 21834002), as well as research Funds of Guangxi University and Central China Normal University.


## REFERENCES


- (1) Trosko, J. E.; Ruch, R. J. *Front. Biosci.* **1998**, *3*, 208–236.
- (2) Gartner, Z. J.; Prescher, J. A.; Lavis, L. D. *Nat. Chem. Biol.* **2017**, *13*, 564–568.
- (3) Song, D.; Yang, D.; Powell, C. A.; Wang, X. *Cell Biol. Toxicol.* **2019**, *35*, 89–93.
- (4) Mathien, M. M.; Martin-Jaular, L.; Lavien, G.; Thery, C. *Nat. Cell Biol.* **2019**, *21*, 9–17.
- (5) Chen, X.; Liang, H.; Zhang, J.; Zen, K.; Zhang, X. Y. *Trends Cell Biol.* **2012**, *22*, 125–132.
- (6) Conti, I.; Varano, G.; Simioni, C.; Laface, I.; Milani, D.; Rimondi, E.; Neri, L. M. *Cell* **2020**, *9*, 220.
- (7) Chevallet, M.; Diemer, H.; Van Dorssealer, A.; Villiers, C.; Rabilloud, T. *Proteomics* **2007**, *7*, 1757–1770.
- (8) Luan, Q.; Cahoon, S.; Wu, A.; Bale, S. S.; Yarmush, M.; Bhushan, A. *Biomed. Microdevices* **2017**, *19*, 101.
- (9) Juan-Colás, J.; Hitchcock, I. S.; Coles, M.; Johnson, S.; Krauss, T. F. *Proc. Natl. Acad. Sci. U. S. A.* **2018**, *115*, 13204–13209.
- (10) Kruss, S.; Landry, M. P.; Ende, E. V.; Lima, B. M. A.; Reuel, N. F.; Zhang, J.; Nelson, J.; Mu, B.; Hilmer, A.; Strano, M. *J. Am. Chem. Soc.* **2014**, *136*, 713–724.
- (11) Liang, R. Q.; Broussard, G. J. *ACS Chem. Neurosci.* **2015**, *6*, 84–93.
- (12) Zeng, S.; Wang, S.; Xie, X.; Yang, S. H.; Wang, H. H. *Anal. Chem.* **2020**, *92*, 15194–15201.
- (13) Dijkstra, R. J.; Scheenen, W. J. J. M.; Eri Dam, N.; Roubos, E. W.; ter Meulen, J. J. *J. Neurosci. Methods* **2007**, *159*, 43–50.
- (14) El-Said, W. A.; Choi, J. W. *Biotechnol. Bioprocess Eng.* **2014**, *19*, 1069–1076.
- (15) Chalapathi, D.; Padmanabhan, S.; Manjithaya, R.; Narayana, C. *J. Phys. Chem. B* **2020**, *124*, 10952–10960.
- (16) Yakushenko, A.; Schnitker, J.; Wolfum, B. *Anal. Chem.* **2012**, *84*, 4613–4617.
- (17) Reinhoud, N. J.; Brouwer, H. J.; van Heerwaarden, L.; Kortebouws, G. A. H. *ACS Chem. Neurosci.* **2013**, *4*, 888–894.
- (18) Shin, M.; Venton, B. J. *Anal. Chem.* **2018**, *90*, 10318–10325.
- (19) Qin, W. W.; Wang, S. P.; Li, J.; Peng, T. H.; Wang, K.; Shi, J. Y.; Fan, C. H.; Li, D. *Nanoscale* **2015**, *7*, 15070–15074.
- (20) Kalkum, M.; Lyon, G. J.; Chait, B. T. *Proc. Natl. Acad. Sci. U. S. A.* **2003**, *100*, 2795–2800.
- (21) Debois, D.; Jourdan, E.; Smargiasso, N.; Thonart, P.; De Pauw, E.; Ongena, M. *Anal. Chem.* **2014**, *86*, 4431–4438.
- (22) Ben-Nissan, G.; Vimer, S.; Warszawski, S.; Katz, A.; Yona, M.; Unger, T.; Peleg, Y.; Morgenstern, D.; Cohen-Dvashi, H.; Diskin, R.; Fleishman, S. J.; Sharon, M. *Commun. Biol.* **2018**, *1*, 213.
- (23) Zhou, L.; Yue, B.; Dearden, D. V.; Lee, E. D.; Rockwood, A. L.; Lee, M. L. *Anal. Chem.* **2003**, *75*, 5978–5983.
- (24) Santos, V. G.; Regiani, T.; Dias, F. F. G.; Romao, W.; Jara, J. L. P.; Klitzke, C. F.; Coelho, F.; Eberlin, M. N. *Anal. Chem.* **2011**, *83*, 1375.
- (25) Tonin, A. P. P.; Polisel, C. B.; Ribeiro, M. A. S.; Moraes, L. A. B.; Visentainer, J. V.; Eberlin, M. N.; Meurera, E. C. *Int. J. Mass Spectrom.* **2018**, *431*, 50–55.
- (26) Magill, P. L.; Rolston, M.; MacLeod, J. A.; Cadle, R. D. *Anal. Chem.* **1950**, *22*, 1174–1177.
- (27) Liu, N.; Liu, Y.; Yang, Y.; He, L.; Ouyang, J. *Anal. Chim. Acta* **2016**, *913*, 86–93.
- (28) Haddad, R.; Milagre, H. M. S.; Catharino, R. R.; Eberlin, M. N. *Anal. Chem.* **2008**, *80*, 2744–2750.
- (29) Hirabayashi, A.; Sakairi, M.; Koizumi, H. *Anal. Chem.* **1994**, *66*, 4557–4559.
- (30) Schäfer, K. C.; Balog, J.; Szaniszló, T.; Szalay, D.; Mezey, G.; Dénes, J.; Bognar, L.; Oertel, M.; Takats, Z. *Anal. Chem.* **2011**, *83*, 7729–7735.
- (31) Liu, N.; Lu, X.; Yang, Y. H.; Yao, C. X.; Ning, B. M.; He, D. C.; He, L.; Ouyang, J. *Talanta* **2015**, *143*, 240–244.
- (32) Teunissen, S. F.; Fernandes, A. M. A. P.; Eberlin, M. N.; Alberici, R. M. *TrAC, Trends Anal. Chem.* **2017**, *90*, 135–141.
- (33) Schwab, N. V.; Porcari, A. M.; Coelho, M. B.; Schmidt, E. M.; Jara, J. L.; Visentainer, J. V.; Eberlin, M. N. *Analyst* **2012**, *137*, 2537–2540.
- (34) Porcari, A. M.; Fernandes, G. D.; Barrera-Arellano, D.; Eberlin, M. N.; Alberici, R. M. *Analyst* **2016**, *141*, 1172.
- (35) Jansson, E. T.; Dulay, M. T.; Zare, R. N. *Anal. Chem.* **2016**, *88*, 6195–6198.
- (36) Autelman, S. M.; Caggiula, A. R. *Science* **1977**, *195*, 646–653.
- (37) Floresco, S. B. *Trends Neurosci.* **2015**, *38*, 465–467.
- (38) Xing, B.; Li, Y. C.; Gao, W. J. *Brain Res.* **2016**, *1641*, 217–233.
- (39) Gallitto, A. A.; Zingales, R.; Battaglia, O. R.; Fazio, C. *Phys. Educ.* **2021**, *56*, No. 025007.
- (40) Schneider, C. A.; Rasband, W. S.; Eliceiri, K. W. *Nat. Methods* **2012**, *9*, 671–675.
- (41) Stolee, J. A.; Vertes, A. *Anal. Chem.* **2013**, *85*, 3592–3598.
- (42) Venter, A. R.; Douglass, K. A.; Shelley, J. T.; Hasman, G.; Honarvar, E. *Anal. Chem.* **2014**, *86*, 233–249.
- (43) Feider, C. L.; Krieger, A.; DeHoog, R. J.; Eberlin, L. S. *Anal. Chem.* **2019**, *91*, 4266–4290.
- (44) Armstrong, J.; Barlow, R. B. *Br. J. Pharmacol.* **1976**, *57*, 501–516.


- (45) Corona-Avendano, S.; Alarcon-Angeles, G.; Rosquete-Pina, G. A.; Rojas-Hernandez, A.; Gutierrez, A.; Ramirez-Silva, M. T.; Romero-Romo, M.; Palomar-Pardave, M. *J. Phys. Chem. B* **2007**, *111*, 1640–1647.
- (46) Naccarato, A.; Gionfriddo, E.; Sindona, G.; Tagarelli, A. *Anal. Chim. Acta* **2014**, *810*, 17–24.
- (47) Shariatgorji, R.; Nilsson, A.; Fridjonsdottir, E.; Strittmatter, N.; Dannhorn, A.; Svenningsson, P.; Goodwin, R. J. A.; Odell, L. R.; Andr n, P. E. *Nat. Protoc.* **2021**, *16*, 3298–3321.
- (48) Greene, L. A.; Tischler, A. S. *Proc. Natl. Acad. Sci. U. S. A.* **1976**, *73*, 2424–2428.
- (49) Westerink, R. H. S.; Ewing, A. G. *Acta Physiol.* **2008**, *192*, 273–285.
- (50) Mandela, P.; Ordulay, G. A. *J. Neurochem.* **2006**, *98*, 1521–1530.
- (51) VirgilioS, F. D.; Milani, D.; Leonn, A.; Meldolesill, J.; Pozzan, T. *J. Biol. Chem.* **1987**, *262*, 9189–9195.
- (52) Craig, R. A. I. I.; Garrison, C. E.; Nguyen, P. T.; Yarov-Yarovoy, V.; Bois, J. D. *ACS Chem. Neurosci.* **2020**, *11*, 418–426.
- (53) Edwards, M. A.; Loxley, R. A.; Williams, A. J.; Connor, M.; Phillips, J. K. *Neurotoxicology* **2007**, *28*, 876–885.
- (54) Zisapel, N.; Laudon, M. *Brain Res.* **1983**, *272*, 378–381.
- (55) Ferre, S.; Fredholm, B. B.; Morelli, M.; Popoli, P.; Fuxe, K. *Trends Neurosci.* **1997**, *20*, 482–487.
- (56) Li, H. L.; Tang, J.; Liu, R. H.; Liu, M.; Wang, B.; Lv, Y. F.; Huang, H. Q.; Zhang, C.; Zhang, W. D. *Rapid Commun. Mass Spectrom.* **2007**, *21*, 869–879.
- (57) Wang, L.; Li, W.; Liu, Y. *Pharmazie* **2008**, *63*, 606–610.



**JACS** Au  
AN OPEN ACCESS JOURNAL OF THE AMERICAN CHEMICAL SOCIETY

 Editor-in-Chief  
**Prof. Christopher W. Jones**  
Georgia Institute of Technology, USA

**Open for Submissions** 

pubs.acs.org/jacsau  ACS Publications  
Most Trusted. Most Cited. Most Read.